IEEE Access
Multidisciplinary | Rapid Review | Open Access Journal

Received November 22, 2020, accepted December 3, 2020, date of publication December 25, 2020, date of current version January 6, 2021.

Digital Object Identifier 10.1109/ACCESS.2020.3047424

Ultra-Wideband Trident Inset-Fed Monopole Antenna With a 3-D Conical Ground

PHILIP AYIKU DZAGBLETEY[1], (Member, IEEE), JIN-YOUNG JEONG[2], AND JAE-YOUNG CHUNG[1], (Senior Member, IEEE)

[1]Electrical and Information Department, Seoul National University of Science and Technology, Seoul 01811, South Korea
[2]ICT Device and Packaging Research Center, Korea Electronics Technology Institute, Bundang 13509, South Korea

Corresponding author: Jae-Young Chung (jychung@seoultech.ac.kr)

This work was supported by the Seoul National University of Science and Technology (SeoulTech) through the Advanced Research Project.

ABSTRACT An ultra-wideband antenna with a conical ground and trident inset feeding structure is presented. The antenna consists of a U-shaped monopole designed on a printed circuit board and a three-dimensional conical aluminium mold, serving as the ground. Low frequency (< 1 GHz) matching is achieved with the trident feed branches by inserting them into the monopole. Simulation studies show that the proposed 3-D conical ground outperforms horizontal or flat-lying ground models in terms of impedance matching bandwidth and radiation pattern omni-directivity. The 3-D ground also helps to stably mount the antenna in a measurement facility. Simulation and measured results presented in this paper demonstrate that the proposed antenna is suitable as a testing antenna with omnidirectional radiation patterns over a broad bandwidth. A 14.6:1 bandwidth ratio (0.56 - 8.2 GHz) has been realized at a voltage standing wave ratio below 2:1 with antenna gain above 2 dBi.

INDEX TERMS Antennas, conical ground, inset feeding, monopole antenna, printed monopole antenna, trident feeding, ultra-wideband antennas.

I. INTRODUCTION

Ultra-wideband (UWB) monopole antennas have been extensively studied during the last two decades after the 3.1 to 10.6 GHz communication band was authorized for commercial use in 2002 [1]. They offer not only stable impedance matching but also omnidirectional radiation patterns over a wide bandwidth; preferred for reliable wireless communication. UWB monopole antennas can be categorized into two prominent designs: the first is monopole with the vertically standing radiator mounted perpendicularly to a metal plate [2]–[7]. The second design has the radiator in-plane with the ground and is mostly implemented with a PCB [8]–[11]. The latter have in recent years been integrated into mobile devices thanks to printed circuit board (PCB) miniaturization techniques with various radiator and ground geometries. Such antennas can attain up to 30:1 impedance bandwidth ratio [8].

A comprehensive study in [12] revealed that most impedance bandwidth enhancement techniques conducted on planar monopoles have been focused mainly on the radiator geometry and/or feedline optimization; all the while limited to either the in-plane printed ground or the horizontal ground. As such, in-plane designs, in particular, have seen impedance enhancements at the expense of reduced antenna gain and a distorted omnidirectional radiation pattern across the entire operating bandwidth. For instance, [11] designed a compact in-plane elliptical monopole on a trapezoidal ground with tapered feedline to achieve a 21.6:1 bandwidth ratio ($0.41 \sim 8.86$ GHz) at voltage standing wave ratio (VSWR) < 2.0. This was achieved at the expense of negative antenna gains at lower frequencies (< 1 GHz) and poor cross-polarization at higher frequencies. The Koch snowflake fractal monopole design by [8] aimed to stabilize the radiation patterns over a 30:1 operating bandwidth ratio from 0.65 to 20 GHz by employing parasitic elements in the ground structure. The antenna nonetheless suffered from zero decibel gain performance at the lower frequencies and distorted patterns in the middle and upper frequencies. Thus, these antennas may not be suitable for applications requiring very stable gain and radiation pattern performance such as testing antennas in an electromagnetic measurement system.

The traditional solution to overcoming the radiation pattern and gain instability of the PCB monopole is the vertically standing monopole with a horizontal ground plate.

The associate editor coordinating the review of this manuscript and approving it for publication was Qingfeng Zhang.

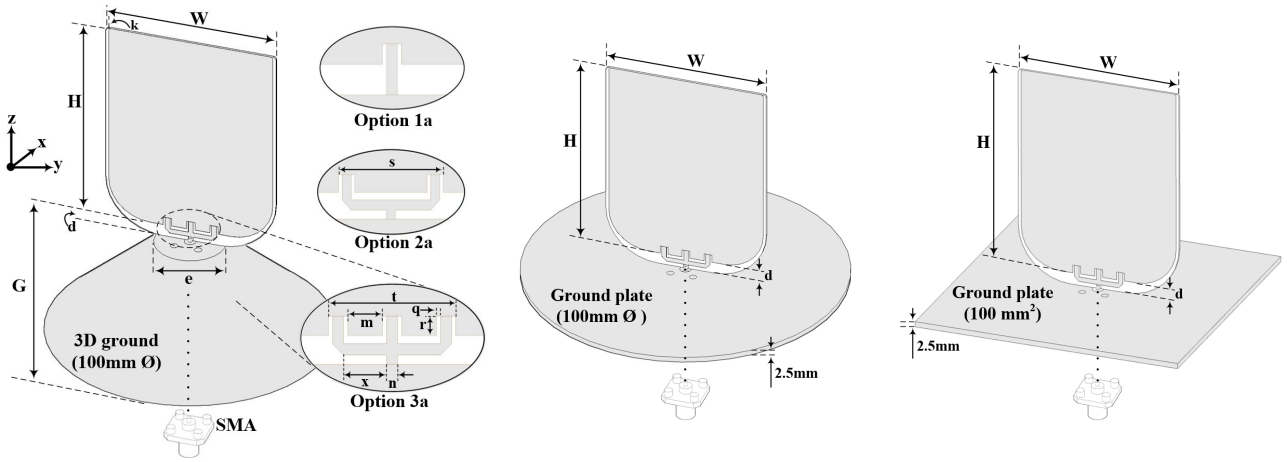

FIGURE 1. Geometry of (a) proposed trident inset-fed monopole antenna with conical ground. Inset Options show different inset feeding methods (b) trident fed monopole antenna with a circular ground (c) trident fed monopole antenna with square ground.

Some modern designs have been proposed in [3]–[6]. However, these have low-frequency impedance drawbacks due to limitations posed by the antenna ground and radiator sizes as reported in [12]. To improve the low-frequency performance, most designs elongate and/or enlarge the feedline and/or ground geometries, as demonstrated in [7] with a large (800 mm diameter) ground plate to obtain a 12.8:1 (0.47 to 6 GHz) bandwidth ratio. Also, [3] designed a tripolarized monopole operating from 1.68 to 4.1 GHz. The monopole is mounted on a 180 mm diameter metal ground to achieve the 84.7% fractional bandwidth (fBW). Other similarly designed monopoles having flat metal grounds such as [4] and [5] also achieved fBWs of 75.1% (1.68-3.7 GHz) and 97.9% (0.6-1.76 GHz). The latter utilized parasitic elements and a 400 mm diameter ground to realize its low-frequency impedance matching. In all these examples, the use of a large metal grounds was prominently implemented to achieve better low-frequency impedance matching. However, a large planar ground is usually not preferred, especially in a measuring chamber, as it increases the overall form factor and blocks the radiations below the ground, thus losing omnidirectional property in the azimuthal plane.

In a related research, [2] improved the low-frequency performance and antenna gain by employing a trident feeding technique on a vertical standing monopole to achieve an 8.1:1 (1.4 to 11.4 GHz) bandwidth ratio. Although this design achieved stable gain and good cross-polarization performance, the low-frequency impedance difficulty persisted. So far, increasing the radiator size and especially the horizontal ground size seems to be the best solution to achieving further low-frequency impedance improvements.

This paper proposes a UWB monopole antenna with broader bandwidth and improved radiation patterns, by employing a new trident inset feed together with a 3-D conical ground. These two techniques which have not been previously reported by any known research; have been shown to enhance low frequency (> 1 GHz) impedance performance while maintaining omnidirectional radiation patterns across the operating bandwidth. The idea is to leverage the strengths of the in-plane PCB monopoles and the vertically standing monopoles to achieve a compact yet improved monopole design. At a VSWR of 2:1 (-9.5dB $S11$), the proposed monopole operates at a 14.6:1 bandwidth ratio from 0.56 to 8.2 GHz. This was achieved with a 61.2 $\times$ 75 mm printed monopole on a 100 $\times$ 35 mm conical metal ground. A stable radiation pattern has also been achieved across the entire bandwidth, with cross-polarization discrimination (XPD) better than 18.56 dB. Details of the radiator and ground design have been presented in Section II. Section III outlines the measured results and performance analysis.

II. ANTENNA DESIGN

The printed monopole as shown in Fig. 1(a) is ellipse-shaped at the base and square-shaped at the top ends. Square-shaped monopoles are most preferred in UWB antenna designs, as they maintain stable radiation patterns across the operating bandwidth [6]. Conversely, the elliptical shape at the base of the radiator enables very smooth surface current distribution on the radiators [13], an important characteristic for low-frequency impedance enhancement.

In this design, the hybrid radiator (elliptical base and square top) was printed on an FR4 substrate ($\varepsilon r = 4.4$, thickness $= 0.8$ mm). Fig. 1(b) and (c) shows the same monopole geometry as 1(a) but with a circular and square metal grounds respectively. This was used as a reference during the conical ground optimization in section II-B. The printed antenna was etched away from the edges of the substrate at $k = 1.2$ mm to further prevent fringed surface currents. This technique was used to obtain a more omnidirectional radiation pattern at the upper cutoff frequency. The monopole (in Fig. 1a) was kept at $W = 61.2$, $H = 75$ mm ($\lambda/4$ @ 0.5 GHz) and $G = 35$ mm throughout the antenna design and optimization process.

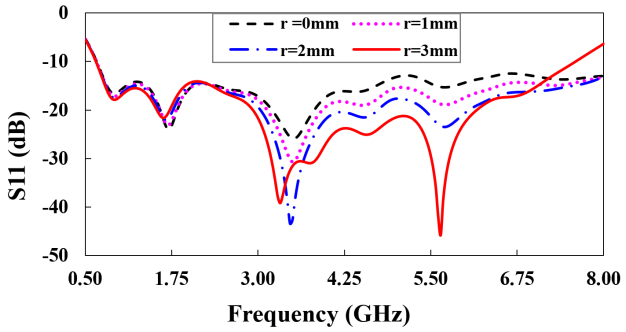

FIGURE 2. Simulated S11 curve of inset feed parameter r mm.

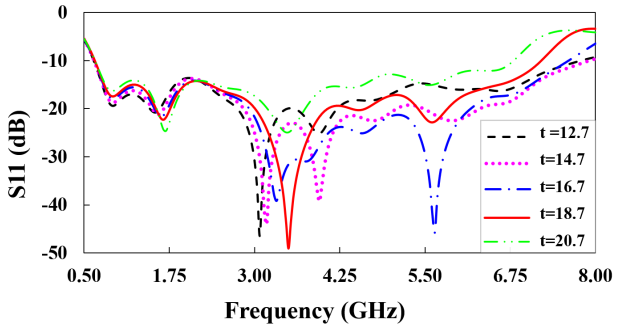

FIGURE 3. Simulated S11 curve of inset feed parameter t mm.

A. TRIDENT INSET FEEDING

The inset feed is a widely known impedance matching technique used in most microstrip antenna and feeding methods [13]. Photo inset *Options 1a* and *2a* in Fig. 1(a) are various known inset feeding methods used in the analysis process. *Option 1a* shows a single-strip inset feedline, *Option 2a* shows a dual-strip inset feeding.

O*ption 3a* shows the proposed trident-shaped inset feeding technique. Much research has been conducted into the effectiveness of the ordinary microstrip trident feeding approach in [2] and [13]; therefore this manuscript will focus on the effectiveness of the inset-feeding method used in the various feeding Options shown in Fig. 1(a).

The single inset-fed *Option 1a* has a 50 Ω width of $n = 1.5$ *mm* and is placed in the center of the radiator, with width W and length H. The radiator is suspended at distance d from the metal ground, to separate the radiator from the ground. This setup differs from the air gap spacing of [2] because of the PCB substrate, which sits on the ground to ensure stability. The feedline is extended by length r into the radiator and separated by distance q to create the inset groove. In *Option 2a*, the two inset branches are identical to that of *Option 1a* and are separated by a distance s and centered on the radiator.

The trident branch feedlines in *Option 3a* are also identical in width and length. Each branch is spaced at distance m and covers a total distance t on the radiator, where $t \approx W/3$.

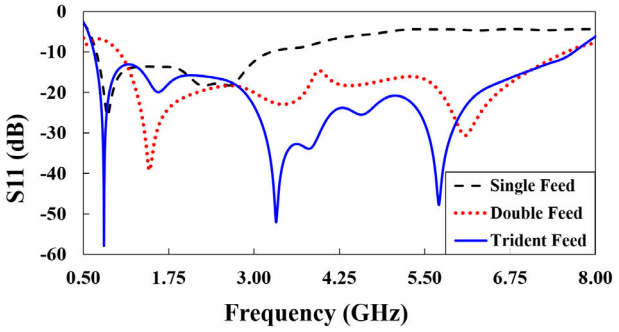

FIGURE 4. Simulated S11 comparison of the 3 inset feeding methods.

TABLE 1. Simulation results comparison of the 3 inset feeding methods.

Feed Option	Parameters (*d, t, r, q*) *mm*	Bandwidth (GHz)	Bandwidth Ratio
1a (Single)	4.5, --, 3.5, 0.74	0.7 - 2.67	3.8
2a (Double)	4, 15.2, 4, 0.76	0.95 - 7.57	7.9
3a (Trident)	4.5, 16.7, 3, 0.65	0.62 - 7.70	12.42

Bandwidth is calculated at -10 dB S11

The inset groove r has a direct relationship with the monopole's resonant input resistance (R_{in}) given in (1).

$$R_{in} = \frac{1}{2\,(G + G_O)} \cos^2\left(\frac{\pi}{H} r\right) \tag{1}$$

$$G = \frac{I_O}{120\pi^2} \,\|G_O = G \cdot I_O\,(k_o L \sin\theta) \tag{2}$$

where G and G_O are the self-conductance and mutual conductance given by (2) respectively. I_O is the approximated surface current density obtained from formulated approximations in [13], and k_o the free-space phase constant. Increasing r towards the center of the patch ($r \approx H/2$) introduces junction capacitances that affect R_{in} and the resonant frequency; causing the $cos^2(\pi r/H)$ function in (1) to increase rapidly with the position of the feedline. Consequently, changing the value of q also affects this junction capacitance and thus useful in obtaining a desirable R_{in} by rigorous optimization.

The distance m between successive inset branches is a function of the maximum allowable feed distance t_{max}. The relationship shown in (3) and (4) holds true in obtaining the initial values for optimization.

$$t_{\max} \approx \frac{W}{3} \Big|_{\,for\, \frac{n}{h_o} > 1} \tag{3}$$

$$2n < m > \frac{t}{3} \Big|_{\,for\; d \leq 2r} \tag{4}$$

where h_o is the substrate thickness given by 0.8 mm. Thus, for the given $W = 61.2$ mm, t can be ideally increased to 20.4 mm, m can range between 3.0 and 6.8. From (1) the initial value of r is set at 3.2 mm for R_{in} of 225.32 Ω.

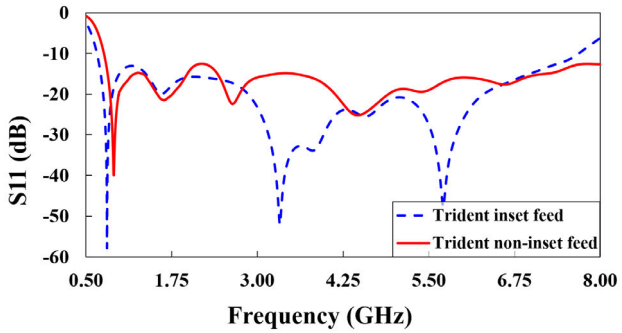

FIGURE 5. Simulated S11 comparison of trident inset and trident non-inset feeds.

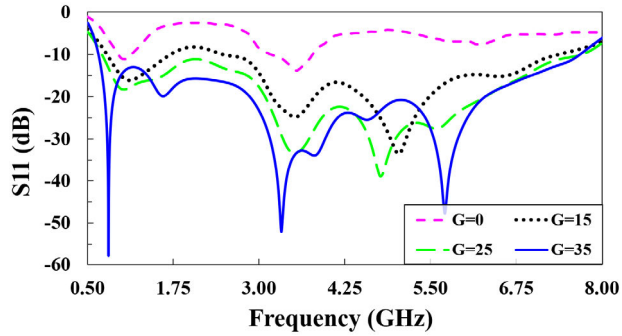

FIGURE 6. Simulated S11 curve of varying ground height (G) mm.

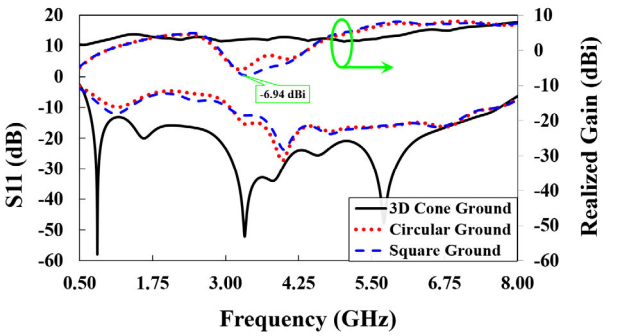

FIGURE 7. Simulated S11 and realized gain (x-y plane) comparisons of 3-D conical ground (Fig. 1a), square flat and circular flat ground (Fig. 1b/c).

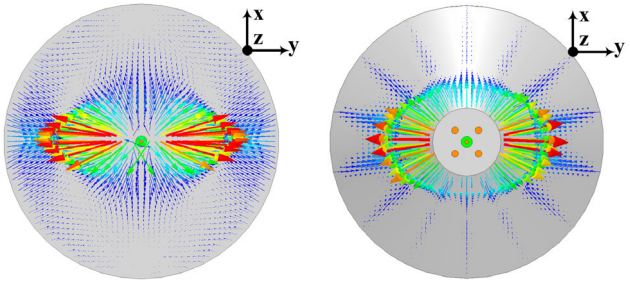

FIGURE 8. Simulated surface current distribution for (a) circular-shaped and (b) 3-D conical shaped grounds. View is from top of antennas at 4.5 GHz.

As noted earlier and from [13], the inset slots introduce reactance properties that enhance input impedance matching. This is controlled by optimizing parameters r and q. Fig. 2 shows the real and imaginary impedance curve when varying r (at $q = 0.65$ mm). The curve, in keeping with equation (1), shows much variation in the imaginary (reactance) curve when r is varied, and q is kept constant. Varying q predominantly changes the capacitance whereas varying r (directly proportional to R_{in} from equation 1) alters the inductance to a larger extent. The optimized values for the proposed design in *Option* 3a were realized at $r = 3$ mm and $q = 0.65$ mm. The parameter q will thus exhibit similar frequency response as r.

Fig. 3 shows the sweep when varying the length t in Fig. 1. Satisfying the condition of equation (4), it can be seen that the optimum value of t lies between 14.7 mm and 18.7 mm, which is $\approx W/3$. The spacing d between the ground layer and metallic radiator as characterized in the constraints of equation 4 is kept at 5 mm to fundamentally prevent galvanic contact between the two surfaces and also to reduce ground to radiator surface current induction. The latter reduces the omnidirectional pattern of the antenna.

Fig. 4 shows the $S11$ curves for the three inset feed options. The key parameters (d, t, r and q) for achieving optimum results in all three options are therefore optimized to obtain the widest possible bandwidth with the same conical ground and radiator size. In *Option 1a*, $d = 4.5$ mm, $r = 3.5$ mm and $q = 0.74$ mm.

In *Option 2a*, $d = 4$ mm, t (or s) $= 15.2$ mm, $r = 4$ mm and $q = 0.76$ mm. In *Option 3a*, $d = 4.5$ mm, $t = 16.7$ mm, $r = 3$ mm and $q = 0.65$ mm. The coupling between the ground plane and the radiator is altered by varying d and t (in *Options 2a* and *3a* only). This changes the input reactance, and thus effective for input impedance matching. Also, altering the inset parameters r and q, introduces additional capacitive and inductive effects, rendering a net cancellation of the input reactance.

Fig. 4 and Table 1 show that the trident inset feed has superior performance compared with the single and double inset feed methods. The bandwidth ratios agree well with [2], which obtained similar results for the single and double non-inset feed methods. Moreover, the inset feeding approach in the single and double feed strips achieved even better results than in [2], [6]. For its single and double feed options, [2] obtained bandwidth ratios of 2.26:1 and 7.52:1 respectively. Whereas the inset methods implemented in this paper obtained a 3.8:1 and 7.9:1 bandwidth ratio for single and double inset-feeds, respectively. It should be noted that, without optimizing the key parameters, the feeding options may operate from the same lowest frequency of 0.62 GHz but will have very small bandwidths. This is because the net reactance offered by each of the three options at the same dimensions, tend to affect only the higher frequency regions.

The proposed trident inset method was compared with a trident non-inset feed design, similar to that of [2]. Both antennas were simulated with the same conical ground and

TABLE 2. Simulation results comparison of the 3 metal grounds.

Ground type	Parameters (*d, t, r, q*) *mm*	Bandwidth (GHz)	Bandwidth Ratio
3-D Cone	4.5, 16.7, 3.0, 0.65	0.62 - 7.70	12.42
Circular	4.8, 16.7, 3.1, 0.62	3.1 - 7.70	2.48
Square	5.0, 17.0, 3.6, 0.75	3.0 - 7.61	2.53

Bandwidth is calculated at −10 dB S11

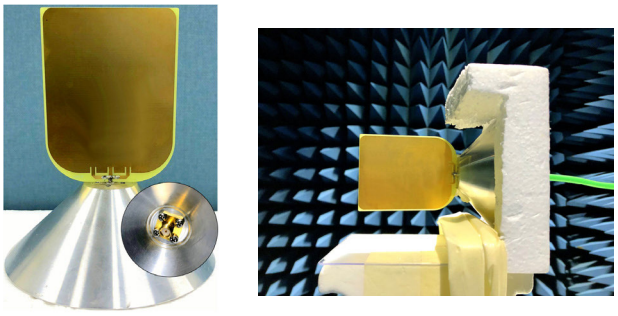

FIGURE 9. Fabricated antenna models. (a) Proposed trident inset-fed antenna. (Inset photo is the backside of the antenna with the SMA port and screws) (b) Proposed antenna in an anechoic chamber with Styrofoam mount.

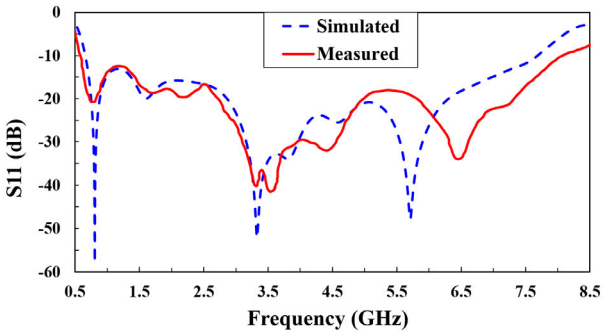

FIGURE 10. Simulated and measured S11 of proposed antenna.

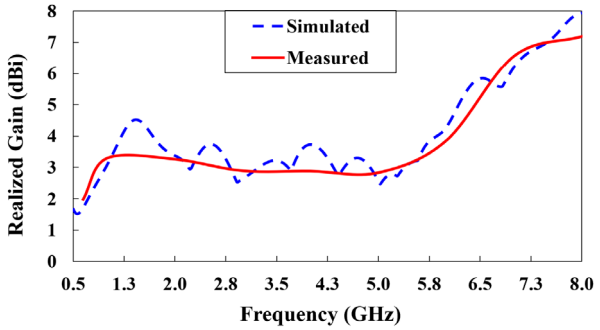

FIGURE 11. Simulated and measured antenna gain of proposed antenna in x-y plane.

radiator size. However, to ensure a fair comparison, the key parameters (d, m and t) for the non-inset trident design were optimized to achieve the best possible impedance matching ($d = 5$ mm, $m = 6.85$ mm and $t = 17.1$ mm). As noted earlier, the inset-fed parameters r and q are essential in achieving a wider impedance bandwidth, as they introduce more reactance cancelling properties.

Fig. 5 shows the simulation comparison of the two antenna types. As can be seen, the lower cutoff frequency for the non-inset method is at 0.754 GHz for −10 dB $S11$, whereas that of the inset method extends to 0.62 GHz. Although the higher frequency cutoff for the non-inset is up to 8.9 GHz as compared to 7.8 GHz for the inset method, it is lacking significantly in the lower frequencies. This is a common challenge for most metal-plate monopoles. The comparison shows that the proposed trident inset method can improve low-frequency impedance matching.

B. 3-D CONICAL GROUND

All the analysis performed on the antennas in Section II-A were with the proposed conical ground. In this section, the design and performance of the conical ground is compared with those of square and circular ground plates, with relatively similar physical dimensions.

In most measurement chambers, a flat ground monopole test antenna poses a challenge when mounting. Complex mounting brackets are used to hold the suspending radiator and the flat ground, to ensure stability during rotation. The use of a conical ground (see Fig. 1a) simplifies the bracket geometry, as the radiator is soldered and firmly screwed to the ground while separated by the PCB, which rests on the ground. The proposed design extends the ground as a mounting bracket, which then minimizes the combined length of the antenna plus mounting bracket. The 3-D cone-shaped ground is an all-metal design with a hollow back and a flat top. The flat-top in Fig. 1a measures $e = 25$ mm with a height G. The ground has a consistent thickness of 2.5 mm.

Fig. 6 shows the $S11$ simulation when G is varied from zero to 35 mm (Fig. 1a). The base of the cone is kept at 100 mm in diameter. It should be noted that at $G = 0$ mm, the ground is the same as the flat circular ground shown in Fig. 1(b) with 2.5 mm thickness. The graph shows that increasing G not only improves the impedance performance across the entire band but also widens the bandwidth at the lower frequencies.

Conversely, increasing the ground heights of the flat-square and circular ground models (graph not shown) results in very minimal changes in impedance matching. The sharp 90 degree ends at the edges of the latter models increases edge-diffractions which renders any increment in their height (thickness) non-effective [13], [14]. At $G = 35$ mm, a bandwidth between 0.56 to 8.15 GHz was achieved at −10 dB $S11$. This inexpensive method of

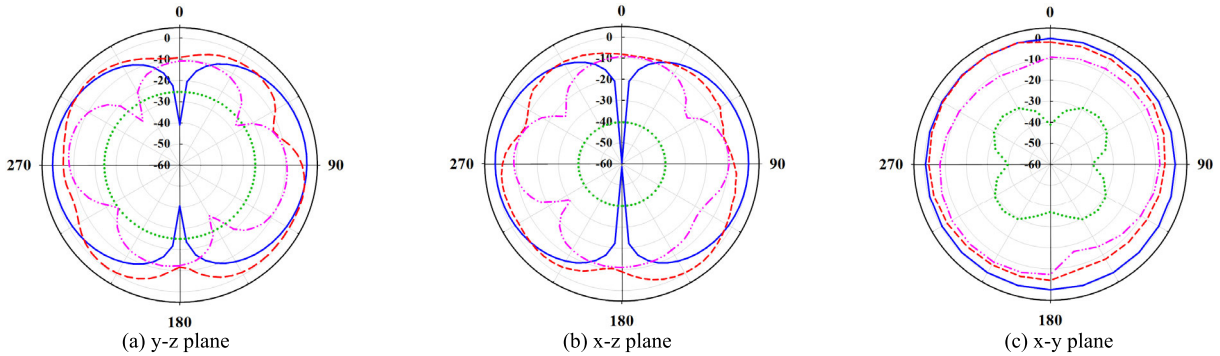

(a) y-z plane (b) x-z plane (c) x-y plane

FIGURE 12. Simulated and measured radiation patterns at 0.65 GHz for the proposed antenna.

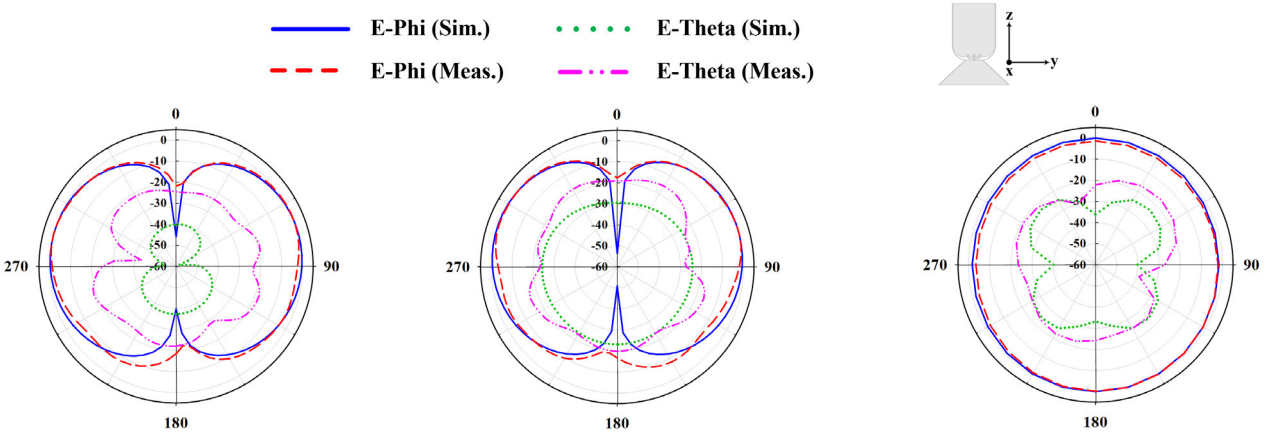

(a) y-z plane (b) x-z plane (c) x-y plane

FIGURE 13. Simulated and measured radiation patterns at 1.0 GHz for the proposed antenna.

increasing the impedance bandwidth is more efficient when compared with the large (800 mm diameter) circular ground in [7], which achieved a 0.47 GHz low-frequency cutoff. The method is also superior to the 150 mm × 150 mm square ground size in [2], which achieved a 1.5 GHz low-frequency cutoff. Therefore, by a relative comparison of antenna size and performance, the proposed structure achieved better low-frequency impedance performance compared with [2] and [7].

Fig. 7 shows the simulated $S11$ and realized gain results for the proposed 3-D conical ground as well as an optimized circular ground and a square metal ground geometry. The key parameters (d, t, r and q) of the feed network were rigorously optimized to obtain the widest possible impedance bandwidth for a fair analysis and comparison. Fig. 1(b) shows the trident inset monopole on a circular ground with 100 mm diameter and 2.5 mm thickness. Using the same radiator size of 61.2 mm × 75 mm, the trident parameters were set to $d = 4.8$ mm, $t = 16.7$ mm, $r = 3.1$ mm and $q = 0.62$ mm. A 100 mm × 100 mm square-shaped ground shown in Fig. 1(c) was also designed with $d = 5.0$ mm, $t = 17.02$ mm, $r = 3.6$ mm, $q = 0.75$ mm, and thickness of 2.5 mm with the same radiator size. The circular and square-shaped grounds showed similar impedance performance with slight variations as shown in Fig. 7. Both grounds obtained bandwidths of 180 MHz and 510 MHz respectively at 1.1 GHz low frequency. The proposed design has a consistently increasing gain (azimuthal plane) with little fluctuations from 1.69 dBi to 7.94 dBi across the 0.5 GHz to 8 GHz. The simulated gain for the circular ground was from −4.9 dBi to 7.3 dBi. That of the square ground also ranged from −4.7 dBi to 7.62 dBi. The circular and flat grounds, however, show significant fluctuations in the gain pattern at the mid and lower frequencies. This may be due to their large radiator-to-ground electrical size ratio; which ideally has to be kept small (larger ground size) in order to achieve a consistent antenna gain result. The proposed model outperformed the circular and square-shaped grounds, although their ground sizes were relatively similar.

The operation of the conical ground is seen more clearly in Fig. 8; with a surface current distribution at 4.5 GHz for the circular-shaped flat and conical grounds. As shown, the current distributes more strongly in the y-z plane, as expected for both models because it is the principal E-plane. However, for the mirror principle of monopole grounds [13] to work effectively, an infinite ground model is required to evenly

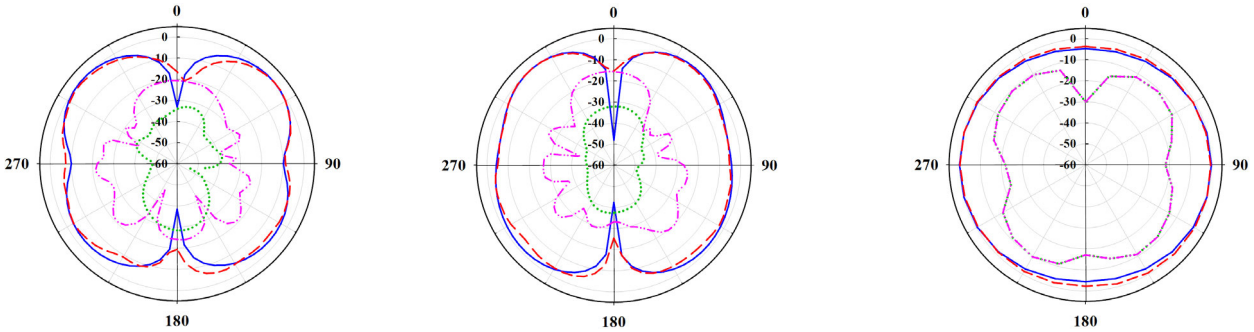

(a) y-z plane (b) x-z plane (c) x-y plane

FIGURE 14. Simulated and measured radiation patterns at 2.0 GHz for the proposed antenna.

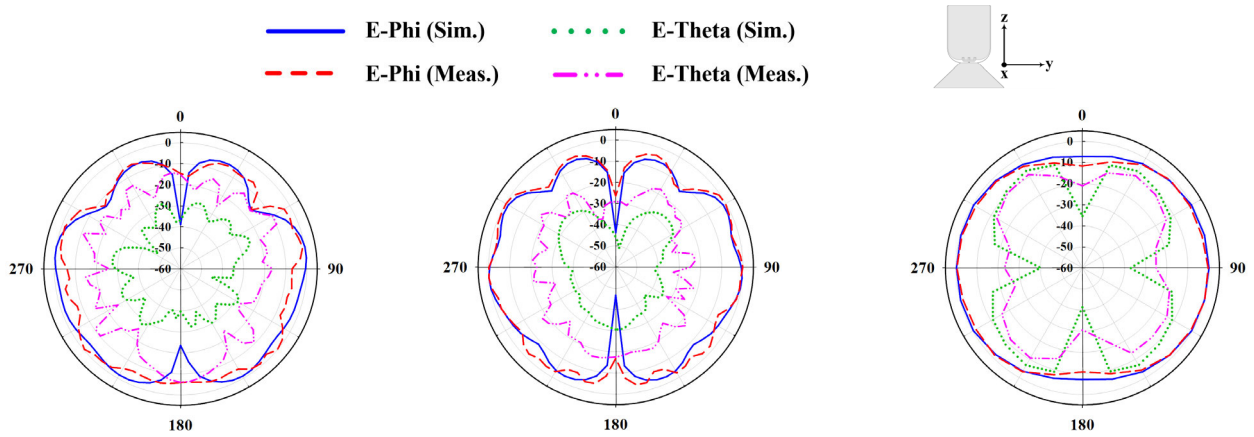

(a) y-z plane (b) x-z plane (c) x-y plane

FIGURE 15. Simulated and measured radiation patterns at 4 GHz for the proposed antenna.

distribute the surface current; ensuring a good radiation pattern and wide impedance bandwidth.

The cone's low elevation angle of 43 degrees at $G = 35$ mm results in a smooth tapered surface, that allows for a more even current distribution on the surface than the flat ground. From Fig. 8b, the conical ground has stronger surface currents forming in the *x*-*z* plane and even current distribution. The flat ground in Fig. 8a shows a higher concentration of surface current in the E-plane (*y*-*z*) plane than the *x*-*z* plane. As will be seen in the next section, this effect makes the 3-D cone a more suitable candidate in tapering radiation patterns for wideband monopole antennas. A summary of the comparisons and optimized parameters are shown in Table 2.

III. MEASUREMENT RESULTS AND DISCUSSIONS

The proposed flat-top conical ground and trident inset-fed radiator were fabricated, measured and analyzed. Fig. 8 shows the conical ground on which the printed radiator is mounted. The ground was machined from a single aluminium metal slab with four 2.6 mm mounting screw holes and a 4.1 mm center hole for a SubMiniature version A (SMA) port. (see inset image of Fig. 9a) The square-flange SMA port with an elongated Teflon receptacle fits into the center portion of the ground, to which it was screwed. The excess Teflon receptacle was cut away, revealing the SMA signal pin, which was soldered to the center microstrip feedline of the trident inset feed network. The fabricated ground was measured at $G = 35$ mm, $e = 25$ mm with a base diameter of 100 mm.

Fig. 9b shows the proposed antenna in an anechoic chamber for far-field measurement. The antenna was held in place by a simple Styrofoam bracket. The lightweight of the aluminium ground, as well as the tapered nature of the cone, ensured a strong fit into the Styrofoam groove. The antenna weighed 96g.

Fig. 10 shows the simulated and measured $S11$ of the proposed antennas. Whereas the simulated bandwidth operated from 0.62 GHz to 7.7 GHz, the measured antenna operated from 0.59 GHz to 8.15 GHz at -10 dB $S11$. This inconsistency may be attributed to unknown simulation errors in the High-Frequency Structure Simulator (HFSS) simulator and/or the modelling. This measured value brings the fractional bandwidth of the proposed antenna to 173% and bandwidth ratio to 13.8:1 (VSWR 1.92:1).

The measured antenna gain curve in Fig. 11 shows a gradual increment of measured gain from 1.98 to 3.3 dBi between 0.65 and 1.0 GHz. The curve shows a consistently

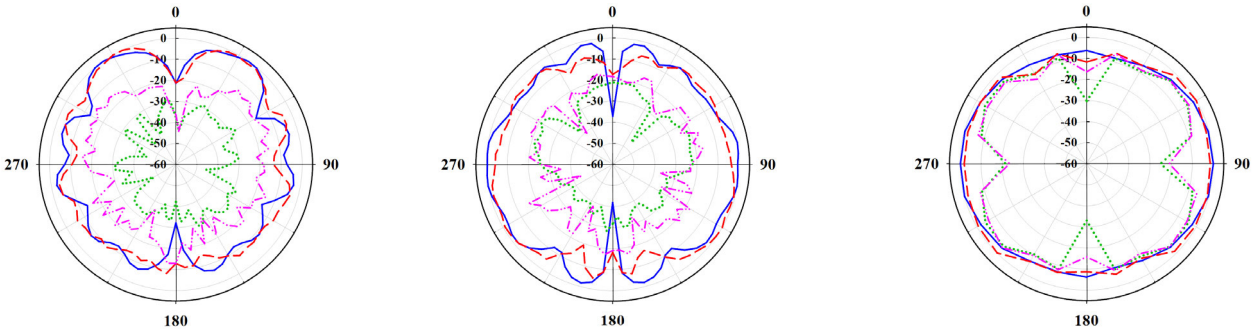

(a) y-z plane (b) x-z plane (c) x-y plane

FIGURE 16. Simulated and measured radiation patterns at 6.0 GHz for the proposed antenna.

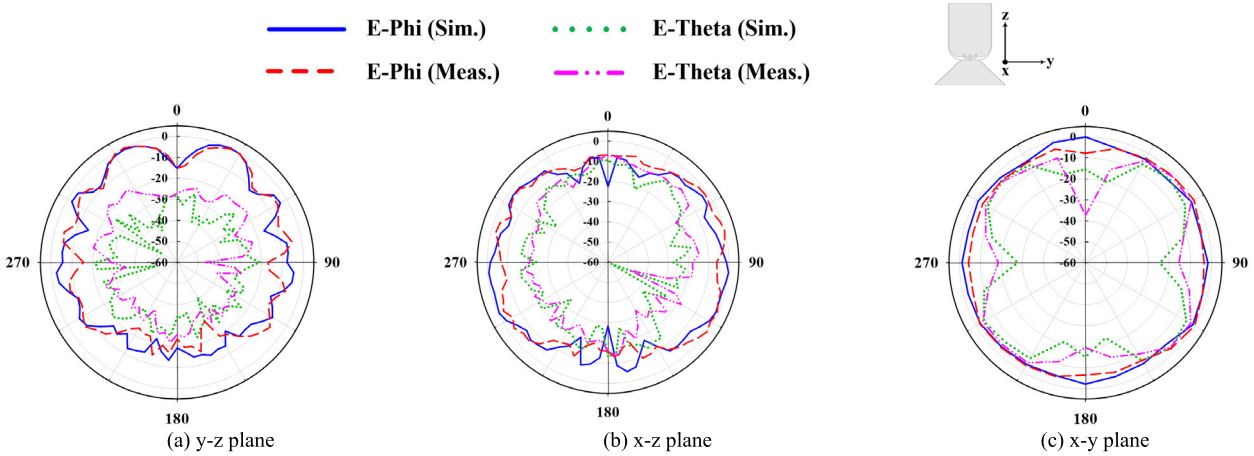

(a) y-z plane (b) x-z plane (c) x-y plane

FIGURE 17. Simulated and measured radiation patterns at 8.0 GHz for the proposed antenna.

TABLE 3. Measured results & geometry comparison of various metal plate monopole antennas with proposed antenna.

Referenced Antenna	Size (mm) Radiator (L × W)	Size (mm) Ground (L × W× H)	Bandwidth (GHz)	BW Ratio / FBW (%)	Gain range (dBi)
[6]	25 × 27.5	Ø 25	3.10 - 10.6	3.4:1 / 109.5	2 - 5
[7]	60 × 100	Ø 800	0.47 - 6.0	12.8:1 / 170.9	---
[2]	40 × 41	150 × 150	1.40 - 11.4	8.1:1 / 156.3	4 - 7
[3]	30 x 100	Ø 180	1.68 - 4.15	2.47:1 / 85.32	3.5 - 8.4
[4]	35 x 36	145 x 145	1.68 - 3.7	2.2:1 / 75.1	6.5 - 8.6
[5]	210 x 125	Ø 400	0.6 - 1.76	2.93:1 / 97.9	0 - 5.5
Proposed Antenna	**80 × 61.2**	**Ø 100 × 35**	**0.56 - 8.2**	**14.6:1 / 174**	**1.98 - 7.19**

Fractional Bandwidth (fBW) is calculated at 2.0 VSWR. L → length. W → width. H → height of ground. Ø → diameter. --- → data not given.

measured gain from 1 to 5 GHz before increasing monotonically to 7.19 dBi at 8 GHz. The gradual increment from low to high is very comparable with existing wideband antenna systems since the radiator-to-ground ratio tends to reduce as the frequency increases. Noting from the mirror principle of monopoles, the electrical size of the ground increases as the wavelength decreases; thus, enabling a higher reflection which results in higher gain in the upper frequencies. The simulated gain shows a slightly jig-sawed curve pattern but is consistent with the measured results. Gain measurements for frequencies below 0.65 GHz are not available because of measurement facility constraints. However, the consistency in the simulation and measured gain implies stable results above 1.0 dBi for frequencies below 0.65 GHz.

A fundamental challenge this research sought to overcome was the distorted radiation patterns that characterize wideband monopole antennas. As noted earlier, previous attempts to overcome this challenge with the use of flat metal grounds have been successful at the expense of antenna size and/or low frequency ($<$ 1 GHz) impedance mismatching. With the low-frequency problem solved using the trident inset feeding method and conical ground, the radiation pattern is also analyzed to verify the structure's performance.

Figures 12 through to 17 show various polar-plotted simulated and measured radiation patterns of the proposed antenna from 0.65 GHz to 8 GHz. All three principal planes of the monopole are shown with both co-polarization (E-Phi) and cross-polarization (E-Theta). For conventional flat metal-ground monopoles, the azimuthal (x-y) plane depends on the operating frequency as noted in [2]. The azimuthal plane predominantly defines the omnidirectional property of the monopole and as such dependent also on the effectiveness of the ground plane in dissipating surface currents. As can be seen in the polar plots, the x-y plane shows a consistent oval-like shape with low cross-polarization.

The y-z and x-z planes also show conformal radiation patterns of the monopole in the intended operating frequency band. In Fig. 12, the 0.65 GHz, in particular, has a slightly larger cross-polarization value than the other frequencies. However, this will not affect the normal performance of the monopole at this frequency due to the rather omnidirectional co-polarization. A nearly consistent oval-shaped pattern is observed in the x-y plane across the measured frequencies. When compared with the simulation patterns, there is much similarity in the curves, except for some curves in the x-z planes of 0.65 GHz and 1 GHz. This can be attributed to the rather small radiator size; being used to achieve this low-frequency performance. The measured results are however conformal. The doughnut shape of the y-z and x-z planes also attest to the performance of the antenna.

Finally, the proposed antenna is compared with previously reported metal plate monopole antennas, shown in Table 3. Square-shaped metal grounds were used by [2] and [4] whereas the others used circular-shaped metal grounds. The proposed antenna demonstrates improved performance with respect not only its size and operating bandwidth but also to the stability of its antenna gain and radiation pattern. [6] for instance achieved good radiation performance at a 3.1 GHz low-frequency cut-off with a 25 mm (4 λ) diameter ground, indicating that it will hypothetically require at least five times its reported ground size to achieve impedance matching at 0.59 GHz. As noted earlier, recent research works such as those reported in [3], [4] and [5] have focused on gain stability improvements with little considerations to improving low-frequency performance without necessarily modifying the ground geometry to achieve compact sizes. Arguably, the bandwidth performance of the proposed design can be attributed to the performance of the trident inset feeding network, the 3-D conical ground and a rather compact radiator size. All three components work together to ensure the impedance bandwidth improvements and radiation patterns as seen in the figures 12 through to 17.

IV. CONCLUSION

A printed monopole antenna with trident inset feeding, mounted on a 3-D conical metal ground, has been proposed and shown to achieve very wide impedance bandwidth with stable gain. The smooth, slanting nature of the conical ground demonstrates an even distribution of surface current on the ground, which in turn enables a more omnidirectional radiation pattern of the monopole across the operating bandwidth. The combined techniques employed in achieving this performance has not been previously reported in the present form and will thus provide an invaluable resource in monopole antenna impedance matching especially in the low frequencies below 1 GHz. The trident inset method can also be applied to other microstrip antennas to improve impedance matching and better current distribution on a radiator.

The proposed design operates well from 0.59 to 8.15 GHz ($-$10 dB $S11$) for antenna gain varying from 1.9 to 7.2 dBi. The low-profile nature of the antenna makes it easy to fabricate and its conical ground enables easy mounting with minimal bracketing required. Although the antenna has a relatively lightweight of 96 g, further work on the 3D conical ground can be investigated to reduce the ground size by using highly polished surfaces and/or metals with higher conductivity. These new materials can thus achieve higher slanting angles with smaller size while maintaining the electrical performance of the ground. The proposed antenna is currently implemented and in use as a test antenna in a compact reverberation chamber for mobile and broadband communication devices.

REFERENCES

[1] *Revision of Part 15 of the Commission's Rules Regarding Ultra-Wideband Transmission Systems ET Docket 98-153*, document FCC 02-48, Federal Communications Commission. (FCC), Washington, DC, USA, 2002.
[2] K.-L. Wong, C.-H. Wu, and S.-W. Su, "Ultrawide-band square planar metal-plate monopole antenna with a trident-shaped feeding strip," *IEEE Trans. Antennas Propag.*, vol. 53, no. 4, pp. 1262–1269, Apr. 2005.
[3] S. X. Ta, D. M. Nguyen, K. K. Nguyen, C. Dao-Ngoc, and N. Nguyen-Trong, "A tripolarized antenna with ultrawide operational bandwidth," *IEEE Trans. Antennas Propag.*, vol. 68, no. 6, pp. 4386–4396, Jun. 2020.
[4] Y. Zhang, Y. Zhang, D. Li, K. Liu, and Y. Fan, "Ultra-wideband dual-polarized antenna with three resonant modes for 2G/3G/4G/5G communication systems," *IEEE Access*, vol. 7, pp. 43214–43221, 2019.
[5] R. Lian, T.-Y. Shih, Y. Yin, and N. Behdad, "A high-isolation, ultra-wideband simultaneous transmit and receive antenna with monopole-like radiation characteristics," *IEEE Trans. Antennas Propag.*, vol. 66, no. 2, pp. 1002–1007, Feb. 2018.
[6] G. Teni, N. Zhang, and J. Qiu, "Research on a novel folded monopole with ultrawideband bandwidth," *IEEE Antennas Wireless Propag. Lett.*, vol. 13, pp. 802–805, 2014.
[7] S.-G. Zhou, J. Ma, J.-Y. Deng, and Q.-Z. Liu, "A low-profile and broadband conical antenna," *Prog. Electromagn. Res. Lett.*, vol. 7, pp. 97–103, 2009.
[8] M. Manohar, "Miniaturised low-profile super-wideband koch snowflake fractal monopole slot antenna with improved BW and stabilised radiation pattern," *IET Microw., Antennas Propag.*, vol. 13, no. 11, pp. 1948–1954, Sep. 2019.
[9] M. A. Ul Haq, S. Koziel, and Q. S. Cheng, "Miniaturisation of wideband antennas by means of feed line topology alterations," *IET Microw., Antennas Propag.*, vol. 12, no. 13, pp. 2128–2134, Oct. 2018.

[10] J. Liu, S. S. Zhong, S. G. Hay, and K. P. Esselle, "Compact super-wideband asymmetric monopole antenna with dual-branch feed for bandwidth enhancement," *Electron. Lett.*, vol. 49, no. 8, pp. 515–516, Apr. 2013.
[11] S.-S. Zhong, X.-L. Liang, and W. Wang, "Compact elliptical monopole antenna with impedance bandwidth in excess of 21:1," *IEEE Trans. Antennas Propag.*, vol. 55, no. 11, pp. 3082–3085, Nov. 2007.
[12] R. Cicchetti, E. Miozzi, and O. Testa, "Wideband and UWB antennas for wireless applications: A comprehensive review," *Int. J. Antennas Propag.*, vol. 2017, pp. 1–45, 2017.
[13] C. A. Balanis, "Microstrip and mobile communications antennas," in *Antenna Theory, Analysis and Design*. Hoboken, NJ, USA: Wiley, 2016, pp. 785–787.
[14] W. Wang, Y. Wang, S. Lou, S. Zhang, and Y. Zhou, "Effect of ground plane deformation on electrical performance of air microstrip antennas," *Int. J. Antennas Propag.*, vol. 2020, Mar. 2020, Art. no. 4029780.

PHILIP AYIKU DZAGBLETEY (Member, IEEE) received the B.Sc. degree in telecommunication engineering from KNUST-Ghana, in 2013, the M.Sc. degree from Hanbat University, in 2016, and the Ph.D. degree from the Department of Electrical and Information Engineering, Seoul-Tech University, in 2020. He is currently an Assistant Research Professor with the Department of Electrical and Information Engineering, Seoul National University of Science and Technology, Seoul Korea. He has completed several projects, including 5G antenna measurement systems, millimeter-wave antenna array systems, and wearable fabric antennas. His research interests include microwave transmit array designs, bioelectromagnetic millimeter-wave antenna systems, and circuit design for industrial and commercial use.

JIN-YOUNG JEONG received the B.S. and M.S. degrees from the Seoul National University of Science and Technology, South Korea, in 2014 and 2017, respectively. Since 2017, he has been with the ICT Device and Packaging Research Center, Korea Electronics Technology Institute (KETI), South Korea, where he has conducted research in RF passive components and modules. His current research interests include microwave passive components, LTCC- and printed circuit board (PCB)-based multilayer modules, Si interposer with IPD, and high-efficiency power amplifiers.

JAE-YOUNG CHUNG (Senior Member, IEEE) received the B.S. degree from Yonsei University, South Korea, in 2002, and the M.S. and Ph.D. degrees from The Ohio State University, USA, in 2007 and 2010, respectively, all in electrical engineering. From 2002 to 2004, he was with Motorola Korea as an RF Engineer. From 2010 to 2012, he worked at Samsung Electronics, South Korea, as an Antenna Engineer. He is currently an Associate Professor with the Department of Electrical and Information Engineering, Seoul National University of Science and Technology, South Korea. His research interests include electromagnetic measurement and antenna design.